Journal of Orthopaedic Research
16:155-162 The Journal of Bone and Joint Surgery, Inc.

Bone Regeneration by Implantation of Purified, Culture-Expanded Human Mesenchymal Stem Cells

*†Scott P. Bruder, ‡Andreas A. Kurth, ‡Marie Shea, ‡Wilson C. Hayes, *Neelam Jaiswal, and *Sudha Kadiyala

**Osiris Therapeutics, Baltimore, Maryland, †Department of Orthopaedics, Case Western Reserve University, Cleveland, Ohio, and ‡Orthopaedic Biomechanics Laboratory, Department of Orthopaedic Surgery, Beth Israel Deaconess Medical Center, and Harvard Medical School, Boston, Massachusetts, U.S.A.*

Summary: Bone marrow contains a population of rare progenitor cells capable of differentiating into bone, cartilage, tendon, and other connective tissues. These cells, referred to as mesenchymal stem cells, can be purified and culture-expanded from animals and humans and have been shown to regenerate functional tissue when delivered to the site of musculoskeletal defects in experimental animals. To test the ability of purified human mesenchymal stem cells to heal a clinically significant bone defect, mesenchymal stem cells isolated from normal human bone marrow were culture-expanded, loaded onto a ceramic carrier, and implanted into critical-sized segmental defects in the femurs of adult athymic rats. For comparison, cell-free ceramics were implanted in the contralateral limb. The animals were euthanized at 4, 8, or 12 weeks, and healing bone defects were compared by high-resolution radiography, immunohistochemistry, quantitative histomorphometry, and biomechanical testing. In mesenchymal stem cell-loaded samples, radiographic and histologic evidence of new bone was apparent by 8 weeks and histomorphometry demonstrated increasing bone formation through 12 weeks. Biomechanical evaluation confirmed that femurs implanted with mesenchymal stem cell-loaded ceramics were significantly stronger than those that received cell-free ceramics. These studies demonstrate that human mesenchymal stem cells can regenerate bone in a clinically significant osseous defect and may therefore provide an alternative to autogenous bone grafts.

During embryologic development, cells of the mesodermal layer give rise to multiple mesenchymal tissue types including bone, cartilage, tendon, muscle, fat, and marrow stroma. These precursor cells, also present in the postnatal organism, are referred to as mesenchymal stem cells (6,36). Recently, techniques for the isolation of adult bone marrow-derived human and animal mesenchymal stem cells have been described (10,18,27,31,37,46), as well as techniques for directing their differentiation into the osteogenic (18,23,26,27), chondrogenic (24,28), tenogenic (7,52), myogenic (47), adipogenic (38), and marrow stromal (32) lineages. These cells have also been shown to retain their developmental potential following extensive subcultivation *in vitro* (4,14,18), thus supporting their characterization as stem cells. Human mesenchymal stem cells have been further characterized by documenting their expression of cell surface and extracellular matrix molecules (3,17,19,33), as well as their secretory cytokine profile under various growth and differentiation conditions (20).

Implantation of culture-expanded mesenchymal stem cells has been demonstrated to effect tissue regeneration in a variety of animal models and depends on local factors to stimulate differentiation into the appropriate phenotype. Achilles tendon (52) and full-thickness articular cartilage defects (16,46) have been repaired in the rabbit, regeneration of normal muscle has been achieved in a mouse model of muscular dystrophy (40), and large segmental bone defects have been repaired in rats (26) and dogs (25). Although the cells used for each of these studies were autologous (or syngeneic) mesenchymal stem cells, the biomatrix used for cell delivery varied according to the anatomic setting. Additional studies have shown that following intravenous injection, these cells can serve as long-lasting precursor cells in bone, cartilage, and marrow, thus suggesting a role for them as vehicles for gene therapy (8,37).

Although rat and canine mesenchymal stem cells have been shown to synthesize structurally competent bone in an orthotopic site (25,26), human mesenchymal stem cells have been shown to form bone only *in*

Received September 12, 1997; accepted January 26, 1998.
Address correspondence and reprint requests to S. P. Bruder at Osiris Therapeutics, 2001 Aliceanna Street, Baltimore, MD 21231, U.S.A. E-mail: SBruder@Osiristx.com

vitro (4,23) and in ectopic implantation sites in immunodeficient mice (18). Because fracture healing and bone repair depend on the ability to amass enough cells at the defect site to form a repair blastema, one therapeutic strategy is to directly administer the precursor cells to the site in need of repair. This approach is particularly attractive in the treatment of patients who have fractures that are difficult to heal or who have a decline in their mesenchymal stem cell repository as a result of age (22,28,39,45), osteoporosis (43), or other metabolic derangement. The goal of the current study was to determine whether purified, culture-expanded human mesenchymal stem cells could regenerate bone at the site of a clinically significant osseous defect.

MATERIALS AND METHODS

Cultivation and Manipulation of Human Mesenchymal Stem Cells

Isolation and culture-expansion of human mesenchymal stem cells from a bone marrow aspirate, obtained from a normal volunteer after informed consent, was conducted as previously described (18,20). Following the initial plating in Dulbecco's modified Eagle medium (Sigma Chemical, St. Louis, MO, U.S.A.) containing 10% fetal bovine serum (BioCell Laboratories, Rancho Dominguez, CA, U.S.A.) from a selected lot (31), nonadherent cells were removed on day 3 at the first change of medium, and fresh medium was replaced twice weekly thereafter. Adherent mesenchymal stem cells represent approximately one in 10^5 nucleated cells originally plated. When culture dishes became nearly confluent, the cells were detached and serially subcultured.

Preparation of Implants

Porous hydroxyapatite/β-tricalcium phosphate ceramic blocks, with a mean pore size of 200-450 μm (generously supplied by Zimmer, Warsaw, IN, U.S.A.), were shaped into cylinders approximately 4 mm in diameter and 8 mm in length with a 1 mm central canal or were cut into cubes 3 mm per side. Mesenchymal stem cell-loaded implants were prepared by incubating human fibronectin-coated hydroxyapatite/β-tricalcium phosphate cubes and cylinders in a 7.5×10^6 cell/ml suspension of first-passage mesenchymal stem cells for 2 hours at 37°C, following the application of a brief vacuum to draw the cell suspension into the pores of the sample, as previously described (26). Uniform adherence of cells deep within the pores was confirmed by scanning electron micrography of representative samples, as published elsewhere (10). Cell-free implants were prepared similarly by incubating fibronectin-coated cylinders in a suspension devoid of cells.

Surgical Model and Experimental Design

The femoral gap surgical model employed here has been used extensively in euthymic rats to study long-bone repair (11-13, 26,30,35,42,44,48,49,51). Briefly, both femurs of Harlan Nude (Hsd:Rh-*rnu*) rats (325 g) were exposed by an anterolateral approach. Athymic rats were used because they have an impaired immune response against xenogeneic implants. A polyethylene fixation plate was attached to each femur by four Kirschner wires and two cerclage wires, and an 8 mm transverse segment of the central diaphysis, along with its adherent periosteum, was removed with use of a rotary osteotomy burr under saline irrigation. Each animal then received a cell-free hydroxyapatite/β-tricalcium phosphate cylinder in one femoral defect, an identical cylinder loaded with human mesenchymal stem cells in the contralateral defect, and a mesenchymal stem cell-loaded hydroxyapatite/β-tricalcium phosphate cube in the subcutaneous tissue of the back. The muscles were apposed, and the fascia and skin were closed in a routine layered fashion. Immediately after euthanasia at 4, 8, or 12 weeks, all specimens were radiographed in a lateral position with use of a high-resolution Faxitron Imaging system (Buffalo Grove, IL, U.S.A.) with an exposure of 35 kVp for 30 seconds. At each of the three time points, the femurs from three of the animals were used for quantitative histomorphometry and samples from one animal were used for immunochemistry. The femurs from the remaining seven animals were harvested at the 12-week time point for biomechanical testing and were subsequently pooled with the three samples originally destined for quantitative histomorphometry. All subcutaneous implants were processed for decalcified histology. In addition to the 19 animals that received implants of hydroxyapatite/β-tricalcium phosphate, three additional animals had bilateral femoral defects that were left empty to confirm the critical-sized nature of this defect in athymic rats. These three animals were killed at 12 weeks, and the femurs were processed for undecalcified histology after radiographic imaging. All procedures involving animals were performed in accordance with a protocol approved by the Institutional Animal Care and Use Committee.

Quantitative Histomorphometry and Immunochemistry

For quantitative histomorphometry, the limbs were fixed, dehydrated, cleared, embedded in polymethylmethacrylate, cut, and ground to a thickness of 100 μm for staining with Toluidine blue-O. Quantitative assessment of bone formation was performed with use of Quantimet 500MC (Leica Cambridge, Cambridge, England) image-analysis software as previously described (26). Specifically, analysis was performed on the area of each section corresponding to the new cortical regions defined by the dimensions of the original implant. Areas of bone, ceramic, and soft tissue were easily distinguished by the image-analysis software on the basis of the difference in color. At the magnifications used, approximately 10 separate fields were required to encompass the entirety of each longitudinal section. The data are presented as the fractional area of bone as a percentage of available pore area, in keeping with the historical precedent for histomorphometry in this type of orthopaedic implant (21,25,42,49).

Limbs from one animal at each time point were also prepared for routine immunostaining by monoclonal antibody 6E2, which distinguishes human cells from rat cells (18). Undecalcified cryosections were incubated with 6E2 supernatant or an irrelevant primary monoclonal antibody control (SB-1) (1), followed by fluorescein isothiocyanate-conjugated goat anti-mouse IgG secondary antibody (GIBCO BRL, Gaithersburg, MD, U.S.A.) diluted 1:500 in phosphate-buffered saline. Subcutaneously implanted samples were fixed in formalin, decalcified, embedded in paraffin, sectioned, stained with Mallory-Heidenhain dye, and evaluated for the presence of bone in the pores of the implant.

Biomechanical Testing

Twelve weeks after implantation, seven animals that had cell-free and mesenchymal stem cell-loaded implants and six control animals that did not undergo the procedure were euthanized for torsion testing of femurs as described in technical detail elsewhere (30). The fixation plate and adherent soft tissue were removed, and the metaphyses of the bones were embedded. The specimens were externally rotated in a custom torsion test apparatus at 6° per second until failure was observed. The displacement and load to failure were recorded, and the values for stiffness and strength were calculated with use of custom software.

Statistical Analysis

To analyze the histomorphometric data, the mesenchymal stem cell-loaded and the cell-free samples from each animal were paired,

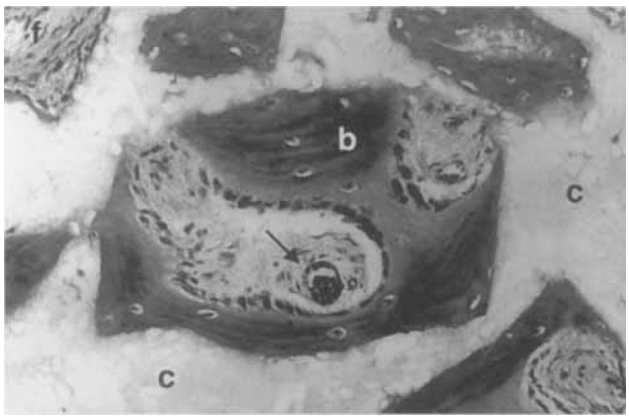

FIG. 1. Light micrograph of a representative histological section from a human mesenchymal stem cell-loaded hydroxyapatite/β-tricalcium phosphate implant placed ectopically in the subcutaneous tissue of an athymic rat. The ceramic phase of the implant (c), which was removed during the decalcification step of histologic processing, can be seen as a granular material. The pores of the implant are filled with bone (b) or blood vessels and fibrous tissue (arrow). Cuboidal osteoblasts are seen lining the surface of the developing bone. (Mallory-Heidenhain, ×75.)

and the data were analyzed by a paired *t* test at each of the three different time points. Because the biomechanical analysis required comparison of three different treatment groups (mesenchymal stem cell-loaded hydroxyapatite/β-tricalcium phosphate implants, cell-free hydroxyapatite/β-tricalcium phosphate implants, and intact controls), one-way analysis of variance with *post hoc* Student-Newman-Keuls tests were used to compare the values for torque, stiffness, and energy to failure for each group.

RESULTS

Mesenchymal Stem Cell-Mediated Osteogenesis in Ectopic Hydroxyapatite/β-Tricalcium Phosphate Implants

Human mesenchymal stem cell-loaded hydroxyapatite/β-tricalcium phosphate cubes implanted in the subcutaneous space of athymic rats displayed evidence of osteogenesis by 4 weeks, but considerably more bone was present within the pores at 8 and 12 weeks. A representative section from a mesenchymal stem cell-loaded cube harvested 12 weeks following implantation is shown in Fig. 1. Bone formation occurs within the pores of the cubes and is associated with vascular elements that penetrate the implant. Such angiogenesis is obligatory to new bone formation, because the secretory activity of osteoblasts is an oriented phenomenon guided by vasculature. As previously demonstrated, the implantation of cell-free cubes (10,18) or of cubes containing normal fibroblastic cells (29,34) always results in the exclusive formation of a fibrovascular tissue within the pores of the ceramic.

Osteotomy Model and Radiography

Figure 2a illustrates the segmental defect model used in this study. The polyethylene fixation plate on top of the femur provides stability following creation of the 8 mm diaphyseal defect. Although a mild, naturally occurring varus deformity was seen in these athymic rats, no gross failure of fixation or other postoperative complications occurred throughout the course of study. However, compromised fixation at euthanasia was found in one animal implanted

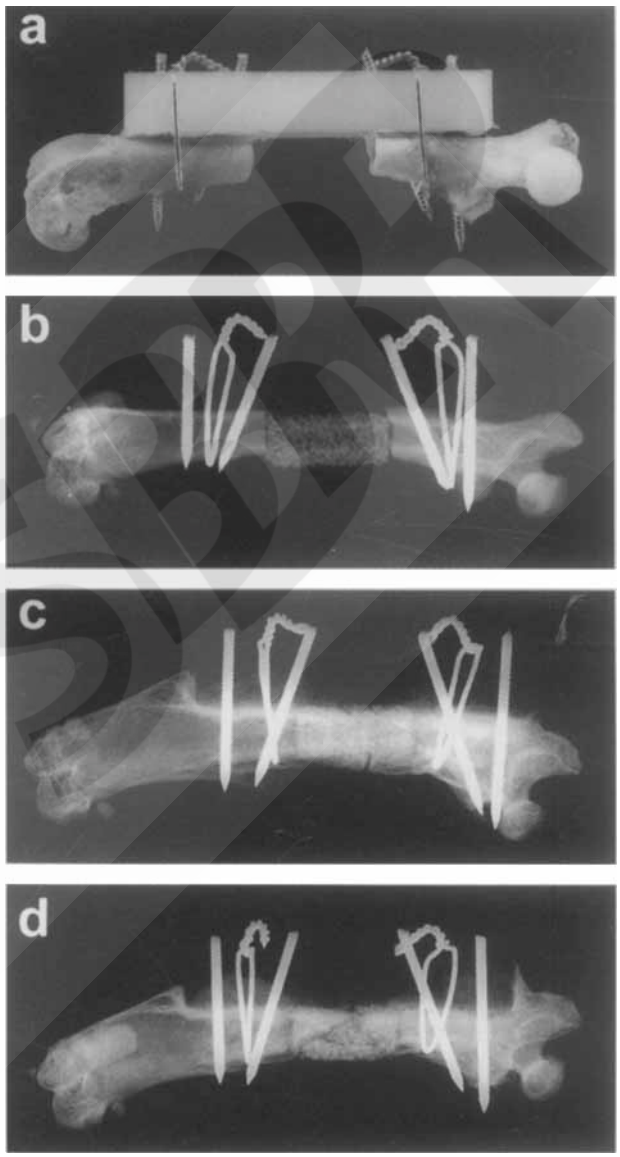

FIG. 2. Segmental gap defect model and radiography. **a:** A polyethylene fixation plate is positioned on the lateral aspect of this representative athymic rat femur. High-resolution radiographs obtained immediately postoperatively (**b**) and following euthanasia at 12 weeks show the pore structure and the extent of healing of the segmental defect with the two implant types, respectively (**c** and **d**). The porous nature of the hydroxyapatite/β-tricalcium phosphate is evident in **b** and serves as a measure against which new bone formation in the pores and at the interface zones can be gauged. Total integration of the implant at the host-ceramic interface is evident in the carrier plus mesenchymal stem cell group (**c**); however, only modest integration is observed in the cell-free implants (**d**). The pores of the mesenchymal stem cell-loaded implant are filled with bone throughout the gap, but the cell-free carrier contains little bone and a centrally located transverse fracture with a butterfly fragment.

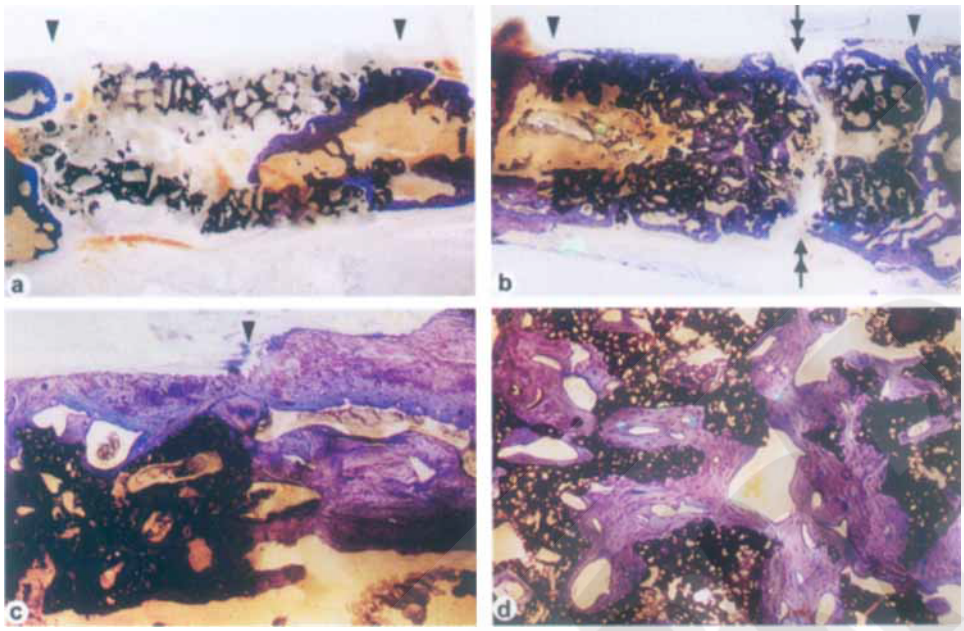

FIG. 3. Histologic representation of bone regeneration in segmental femoral defects. Light micrographs showing representative healing of a segmental defect implanted with a hydroxyapatite/β-tricalcium phosphate carrier alone (**a**) or the carrier plus human mesenchymal stem cells (**b-d**), 12 weeks after implantation. The ceramic appears black in these photomicrographs as an artifact of undecalcified specimen preparation, and bone present within the pores or at the host-implant interface appears blue-violet. The mesenchymal stem cell-loaded specimen shown here was subjected to destructive mechanical torsion testing, processed for histology in two separate pieces, and repositioned to approximate the appearance of the femur prior to testing (**b**). The actual fracture plane is denoted by the double arrows above and below the implant. The cut edges of the host cortices are noted by arrowheads in **a** and **b**. Higher power micrographs demonstrate the substantial amount of bone present at the host-implant interface (**c**) and within the body of the implant (**d**). (Toluidine blue-O; **a** and **b**: ×7, **c**: ×31, and **d**: ×45.)

with mesenchymal stem cell-loaded hydroxyapatite/β-tricalcium phosphate cylinders and cell-free hydroxyapatite/β-tricalcium phosphate cylinders; hence, the samples from this animal were excluded from the study. Control femoral defects that were left empty gave rise to a nonunion, as established by other investigators using euthymic rats (11,26,45). High-resolution Faxitron radiographs provided sufficient clarity and detail to discern subtle changes occurring within the implant and the surrounding host bone. Increasing radiodensity and obliteration of the apparent pore structure seen clearly in the radiographs obtained immediately postoperatively (Fig. 2b) were used as indications of new bone formation within the pores of the implant. Representative radiographs of the femurs from the groups recovered 12 weeks after implantation demonstrate substantially more bone in animals that received mesenchymal stem cell-loaded hydroxyapatite/β-tricalcium phosphate cylinders (Fig. 2c) than in those that received cell-free cylinders (Fig. 2d). Although integration of the implant, or union, was not generally observed by 4 weeks, the subsequent formation of a radiodense bone bridge between the implant and the host at 8 weeks completely masked the interface. By 8 weeks, the mesenchymal stem cell-loaded implants contained considerable bone within the pores and were integrated with the host bone at the ends of the implant. At 12 weeks, union was complete and additional bone was evident in the pores. Callus formation along the fixation plate was observed in some samples, as was an occasional eccentric spicule of bone usually present along the medial aspect of the femur.

Histologic Evaluation

Analysis of the samples stained with Toluidine blue-O confirmed the observations made by radiography. Photomicrographs of representative sections of the implant groups recovered at 12 weeks are shown in Fig. 3. In defects fitted with the hydroxyapatite/β-tricalcium phosphate carrier alone, the pores of the implant were predominantly filled with fibrous tissue even at 12 weeks. Several samples had evidence of modest integration at the host-implant interfaces, and at one end of this representative implant (Fig. 3a), host-derived endosteal bone appears to be advancing into the medullary canal of the carrier as a result of osteoconduction. None of the cell-free ceramic carriers contained bone throughout the pores of the implant.

Most of the pores of the implants loaded with mesenchymal stem cells contained substantial new bone by 8 weeks, and this process of bone regeneration continued through the 12-week assessment period (Fig. 3b). Evaluation of limbs following biomechanical testing indicates that the fractures were of a trans-

TABLE 1. *Bone fill in hydroxyapatite/β-tricalcium phosphate implants as a percentage of available space (mean ± SD)*

	4 weeks (n = 3)	8 weeks (n = 3)	12 weeks (n = 8)
Carrier alone	1.88 ± 0.83	12.95 ± 5.35	30.28 ± 10.18
Carrier + mesenchymal stem cells	2.01 ± 1.85	22.88 ± 4.25[a]	45.77 ± 14.56[b]

[a] P = 0.05 compared with the carrier alone at each time point, as determined by paired *t* tests.
[b] P = 0.001 compared with the carrier alone at each time point, as determined by paired *t* tests.

verse or spiral nature and were generally propagated through a central region of the implant containing cartilage or a modest amount of bone. During the regenerative process, substantial new bone formation occurred at the interface between the host and the implant, leading to a continuous span of bone across the defect. New woven and lamellar bone can be seen in intimate contact with the cut edge of the host cortex at 12 weeks (Fig. 3c), and this region of union is directly contiguous with bone formed throughout the pores of the implant. In regions deeper within the hydroxyapatite/β-tricalcium phosphate (Fig. 3d), filling of the pores with new bone and vasculature is evident. Immunocytochemical staining with antibody 6E2 demonstrated that at 4 weeks, virtually all the cells within the pores of the implant were reactive and, therefore, were of human origin (data not shown). Samples from later time points, which contained substantial amounts of bone, were not amenable to testing because the sensitivity of the antigen-antibody interaction requires the use of unfixed frozen sections, which of course cannot be obtained from such mineralized bone samples.

Histomorphometric Evaluation

The results that have been qualitatively described are mirrored in the histomorphometric data in Table 1. Bone present in the cell-free hydroxyapatite/β-tricalcium phosphate implants primarily represents the osseous ingrowth from the cut ends of the host cortices. At 8 weeks and longer, the mesenchymal stem cell-loaded samples contained significantly more bone than did the cell-free group, and the average bone fraction within the implant increased over time, reaching 22.9 and 45.8% by the 8 and 12-week time points, respectively. This increased bone fraction at 8 weeks is 1.8-fold higher than that measured in cell-free implants at the same time, and, by 12 weeks, is more than 23-fold higher than that observed in either condition at 4 weeks. The volume fraction of the hydroxyapatite/β-tricalcium phosphate carrier remained constant and served as an internal control for histomorphometry. Samples from one animal were not included in the 12-week histomorphometric analysis because mechanical testing shattered one limb in such a way as to prevent reconstruction in an anatomically correct manner; this left eight pairs of limbs available for analysis at the 12-week time point.

Mechanical Testing

Table 2 summarizes the mechanical testing results in terms of torsional strength, stiffness, and total energy absorbed. These results demonstrate increases to 215, 245, and 212% of strength, stiffness, and torsional energy absorbed, respectively, in mesenchymal stem cell-loaded samples compared with cell-free carrier samples. The three groups were found to be statistically different from each other in failure torque and stiffness.

DISCUSSION

The results presented here demonstrate that purified, culture-expanded human mesenchymal stem cells are capable of healing a clinically significant bone defect in a well established model for bone repair. The basic phenomenon of osteogenic differentiation of human mesenchymal stem cells has been proven by the formation of bone in subcutaneous implants in mice (18) and in studies of isolated mesenchymal stem cells *in vitro* (4,23); however, this is the first demonstration that human mesenchymal stem cells can regenerate bone at a clinical site in need of repair, to our knowledge. The combination of mesenchymal stem cells and a porous hydroxyapatite/β-tricalcium phosphate car-

TABLE 2. *Mechanical properties of rat femurs 12 weeks after implantation (mean ± SD)*

	Intact control (n = 11)	Carrier alone (n = 6)	Carrier + mesenchymal stem cells (n = 6)
Strength (N • mm)	409 ± 71	74 ± 63	159 ± 37
Stiffness (N • mm/deg)	39 ± 5.5	6.6 ± 4.2	16.2 ± 4.0
Energy (N • mm × deg)	2.6 ± 0.7	0.6 ± 0.4	1.3 ± 0.8

One-way analysis of variance on each of the parameters showed a significant difference between the groups at $p < 0.0001$. Furthermore, each of the groups was significantly different from the other for strength and stiffness ($p < 0.05$), as determined by *post hoc* Student-Newman-Keuls tests.

rier possesses regenerative potential that is histomorphometrically and biomechanically superior to the carrier alone. This investigation paves the way for the clinical application of autologous mesenchymal stem cell therapy for the treatment of orthopaedic defects in humans.

The progressive increase in radiodensity of the healing bone at 8 weeks parallels the histological observations of processed limbs. Immunocytochemistry proves that the cells associated with the ceramic at 4 weeks are of human origin and that the cells surrounding the implant are from the host. It has been shown that the bone produced by these mesenchymal stem cells is eventually replaced by bone derived from host cells through the normal remodeling sequence (8,15). It is important to note that in the process of healing this osseous defect, bone formation occurs by a direct conversion of mesenchymal cells into osteoblasts rather than by an endochondral cascade. This observation is consistent with previous studies of osteogenesis in implants loaded with animal or human mesenchymal stem cells (10,18,25-27). As the regenerative process continues, the pores of the ceramic are filled with an increasing amount of bone, which is laid down on the walls of the implant or existing bone and oriented by the invading vasculature that provides a portal for the entry and establishment of new marrow islands containing hematopoietic elements and host-derived mesenchymal stem cells. Although we did observe cartilage in a few samples at the biomechanical fracture site, we believe that cells differentiated into chondrocytes as a result of early microfractures within the implant itself, leading to micro-instability and disruption of vascular elements. These environmental cues are known to promote the formation of a cartilaginous callus at the site of healing bones, and this region represents the portion of the implant most likely to fail at mechanical testing.

The presence of bone in the subcutaneously implanted cubes demonstrates that these athymic animals are indeed capable of supporting osteogenic differentiation of human mesenchymal stem cells. However, the rate of bone regeneration is lower than that observed in euthymic rats implanted with syngeneic mesenchymal stem cells (10,26,31) or in severe combined immune deficiency (SCID) mice implanted with human mesenchymal stem cells (data not shown); this suggests that immunocompromised rats are not the optimal hosts for assessment of the bone-forming potential of human mesenchymal stem cells. This may be due in part to the xenogeneic nature of the implant and the increased natural killer cell activity, which may be a compensatory mechanism for the host animal to cope with its deficient T-cell-mediated immunity (41). Nevertheless, a significantly higher amount of bone was formed in the defect that received mesenchymal stem cells than in those limbs that received the carrier only. The extent of host-implant union was greater in the mesenchymal stem cell-loaded implants, which likely reflects the combined contributions of implanted mesenchymal stem cells and host-derived cells.

The ability of human mesenchymal stem cells to regenerate bone in this experimental model compares favorably with other investigations testing implants such as demineralized bone matrix, bone marrow, purified or recombinant bone morphogenetic proteins (BMPs), allograft, ceramics, fibermetals, and gene-activated matrices (11-13,30,35,42,44,48,49,51). In addition to forming a substantial amount of histologically normal bone, the biomechanical data demonstrate that torsional strength and stiffness at 12 weeks were approximately 40% that of intact control limbs; this is more than twice that observed with the cell-free carrier and also twice that achieved in a similar study of bone repair using fresh autograft in a primate long-bone defect model (9).

Recently, growth factors such as recombinant human BMP have been implanted in experimental bone defect models to stimulate bone repair (9,30,51). Although recombinant BMPs are capable of inducing the endochondral cascade in ectopic implants (50), their ability to reproducibly direct bone formation at orthotopic sites has been hampered by the problems associated with the design and selection of an appropriate carrier. In contrast to the mechanical data showing significant bone regeneration in a mesenchymal stem cell-loaded ceramic, purified BMP delivered in the same hydroxyapatite/β-tricalcium phosphate carrier did not increase the strength of the implant compared with the carrier alone (42), even though BMP delivered in alternative carriers induces the formation of structurally competent bone (9,30). The incomplete interconnectivity of pores within this ceramic, combined with its slow resorption and complex geometric structure, may explain why even in the presence of significant bone formation, mechanical strength remains less than that in intact limbs. In addition, stress-shielding of the new bone, as a result of the load-bearing fixation plate, also restricts the strength of the healing defect. We believe, as has been previously suggested (5), that the use of an osteosupportive hydroxyapatite/β-tricalcium phosphate cylinder may not be the optimal matrix for replacement of diaphyseal defects; however, its use in this study confirms that human mesenchymal stem cells are capable of regenerating bone in the site of a large defect. The design of an optimal biomatrix carrier for the delivery of mesenchymal stem cells is an active area of investigation.

Implantation of culture-expanded autologous mesenchymal stem cells offers the advantage of directly

delivering the cellular machinery responsible for synthesizing new bone and circumventing the otherwise slow steps leading to bone repair. Even in patients whose connective tissue has a reduced ability to regenerate, presumably due to a low titer of endogenous mesenchymal stem cells (2,22,28,43,48), these rare mesenchymal stem cells may be isolated, cryopreserved, and culture-expanded over one billion-fold without a loss in their osteogenic potential (4), thus restoring or enhancing the ability of tissue defects to heal in clinical patients. The studies presented here suggest that mesenchymal stem cell-based therapies will be useful for the reconstruction of a variety of bone defects in humans.

Acknowledgment: The authors wish to thank James Cole, Deborah Miller, Jessie Chou, and Diane Sterchi for outstanding technical support. We also thank Dr. Joseph Lane and Dr. Marshall Urist for encouraging this line of investigation, Stephen Haynesworth for providing antibody 6E2, Nozomu Inoue for sharing his Faxitron Imaging system, Kam Leong for constructive comments, and Daniel Marshak for critical reading of the manuscript. This study was supported by Osiris Therapeutics.

REFERENCES

1. Bruder SP, Caplan AI: A monoclonal antibody against the surface of osteoblasts recognizes alkaline phosphatase isoenzymes in bone, liver, kidney, and intestine. *Bone* 11:133-139, 1990
2. Bruder SP, Fink DJ, Caplan AI: Mesenchymal stem cells in bone development, bone repair, and skeletal regeneration therapy. *J Cell Biochem* 56:283-294, 1994
3. Bruder SP, Horowitz MC, Mosca JD, Haynesworth SE: Monoclonal antibodies reactive with human osteogenic cell surface antigens. *Bone* 21:225-235, 1997
4. Bruder SP, Jaiswal N, Haynesworth SE: Growth kinetics, self-renewal, and the osteogenic potential of purified human mesenchymal stem cells during extensive subcultivation and following cryopreservation. *J Cell Biochem* 64:278-294, 1997
5. Bucholz RW, Carlton A, Holmes RE: Hydroxyapatite and tricalcium phosphate bone graft substitutes. *Orthop Clin North Am* 18:323-334, 1987
6. Caplan AI: Mesenchymal stem cells. *J Orthop Res* 9:641-650, 1991
7. Caplan AI, Fink DJ, Goto T, Linton AE, Young RG, Wakitani S, Goldberg VM, Haynesworth SE: Mesenchymal stem cells and tissue repair. In: *The Anterior Cruciate Ligament: Current and Future Concepts*, pp 405-417. Ed by DW Jackson. New York, Raven Press, 1993
8. Caplan AI, Bruder SP: Cell and molecular engineering of bone regeneration. In: *Textbook of Tissue Engineering*, pp 603-618. Ed by R Lanza, R Langer, and W Chick. Georgetown, RG Landes, 1997
9. Cook SD, Wolfe MW, Salkeld SL, Rueger DC: Effect of recombinant human osteogenic protein-1 on healing of segmental defects in non-human primates. *J Bone Joint Surg [Am]* 77:734-750, 1995
10. Dennis JE, Haynesworth SE, Young RG, Caplan AI: Osteogenesis in marrow-derived mesenchymal cell porous ceramic composites transplanted subcutaneously: effect of fibronectin and laminin on cell retention and rate of osteogenic expression. *Cell Transplant* 1:23-32, 1992
11. Einhorn TA, Lane JM, Burstein AH, Kopman CR, Vigorita VJ: The healing of segmental bone defects induced by demineralized bone matrix: a radiographic and biomechanical study. *J Bone Joint Surg [Am]* 66:274-279, 1984
12. Fang J, Zhu YY, Smiley E, Bonadio J, Rouleau JP, Goldstein SA, McKauley LK, Davidson BL, Roessler BJ: Stimulation of new bone formation by direct transfer of osteogenic plasmid genes. *Proc Natl Acad Sci U S A* 93:5753-5758, 1996
13. Feighan JE, Davy D, Prewett AB, Stevenson S: Induction of bone by a demineralized bone matrix gel: a study in a rat femoral defect model. *J Orthop Res* 13:881-891, 1995
14. Goshima J, Goldberg VM, Caplan AI: The osteogenic potential of culture-expanded rat marrow mesenchymal cells assayed in vivo in calcium phosphate ceramic blocks. *Clin Orthop* 262:298-311, 1991
15. Goshima J, Goldberg VM, Caplan AI: The origin of bone formed in composite grafts of porous calcium phosphate ceramic loaded with marrow cells. *Clin Orthop* 269:274-283, 1991
16. Grande DA, Southerland SS, Manji R, Pate DW, Schwartz SE, Lucas PA: Repair of articular cartilage defects using mesenchymal stem cells. *Tissue Eng* 1:345-353, 1995
17. Haynesworth SE, Baber MA, Caplan AI: Cell surface antigens on human marrow-derived mesenchymal cells are detected by monoclonal antibodies. *Bone* 13:69-80, 1992
18. Haynesworth SE, Goshima J, Goldberg VM, Caplan AI: Characterization of cells with osteogenic potential from human marrow. *Bone* 13:81-88, 1992
19. Haynesworth SE, Baber MA, Caplan AI: Characterization of the unique mesenchymal stem cell phenotype in vitro. *Trans Orthop Res Soc* 20:7, 1995
20. Haynesworth SE, Baber MA, Caplan AI: Cytokine expression by human marrow-derived mesenchymal progenitor cells in vitro: effects of dexamethasone and IL-1 alpha. *J Cell Physiol* 166:585-592, 1996
21. Holmes RE, Bucholz RW, Mooney V: Porous hydroxyapatite as a bone graft substitute in diaphyseal defects: a histometric study. *J Orthop Res* 5:114-121, 1987
22. Inoue K, Ohgushi H, Yoshikawa T, Okumura M, Sempuku T, Tamai S, Dohi Y: The effect of aging on bone formation in porous hydroxyapatite: biochemical and histological analysis. *J Bone Miner Res* 12:989-994, 1997
23. Jaiswal N, Haynesworth SE, Caplan AI, Bruder SP: Osteogenic differentiation of purified, culture-expanded human mesenchymal stem cells in vitro. *J Cell Biochem* 64:295-312, 1997
24. Johnstone B, Yoo JU, Barry FP: In vitro chondrogenesis of bone marrow-derived mesenchymal cells. *Trans Orthop Res Soc* 21:65, 1996
25. Kadiyala S, Kraus KH, Bruder SP: Canine mesenchymal stem cell-based therapy for the regeneration of bone. *Trans Tissue Eng Soc* 1:20, 1996
26. Kadiyala S, Jaiswal N, Bruder SP: Culture-expanded, bone marrow-derived mesenchymal stem cells can regenerate a critical-sized segmental bone defect. *Tissue Eng* 3:173-185, 1997
27. Kadiyala S, Young RG, Thiede MA, Bruder SP: Culture expanded canine mesenchymal stem cells possess osteochondrogenic potential in vivo and in vitro. *Cell Transplant* 6:125-134, 1997
28. Kahn A, Gibbons R, Perkins S, Gazit D: Age-related bone loss: a hypothesis and initial assessment in mice. *Clin Orthop* 313:69-75, 1995
29. Kuznetsov SA, Krebsbach PH, Satomura K, Kerr J, Riminucci M, Benayahu D, Robey PG: Single-colony derived strains of human marrow stromal fibroblasts form bone after transplantation in vivo. *J Bone Miner Res* 12:1335-1347, 1997
30. Lee SC, Shea M, Battle MA, Kozitza K, Ron E, Turek T, Schaub RG, Hayes WC: Healing of large segmental defects in rat femurs is aided by rhBMP-2 in PLGA matrix. *J Biomed Mater Res* 28:1149-1156, 1994
31. Lennon DP, Haynesworth SE, Bruder SP, Jaiswal N, Caplan AI: Development of a serum screen for mesenchymal progenitor cells from bone marrow. *In Vitro Cell Dev Biol* 32:602-611, 1996
32. Majumdar MK, Thiede MA, Mosca JD, Moorman MK, Gerson SL: Phenotypic and functional comparison of cultures of marrow-derived mesenchymal stem cells (MSCs) and stromal cells. *J Cell Physiol* 176:57-66, 1998
33. Mosca JD, Majumdar MK, Hardy WB, Pittenger MF, Thiede MA: Initial characterization of the phenotype of the human mesenchymal stem cells and their interaction with cells of the hematopoietic lineage [abstract]. *Blood* 88:186a, 1997

34. Nakahara H, Goldberg VM, Caplan AI: Culture-expanded human periosteal-derived cells exhibit osteochondral potential in vivo. *J Orthop Res* 9:465-476, 1991
35. Ohgushi H, Goldberg VM, Caplan AI: Repair of bone defects with marrow cells and porous ceramic: experiments in rats. *Acta Orthop Scand* 60:334-339, 1989
36. Owen M: Lineage of osteogenic cells and their relationship to the stromal system. In: *Bone and Mineral Research/3*, pp 1-25. Ed by WA Peck. New York, Elsevier, 1985
37. Pereira RF, Halford KW, O'Hara MD, Leeper DB, Sokolov BP, Pollard MD, Bagasra O, Prockop DJ: Cultured adherent cells from marrow can serve as long-lasting precursor cells for bone, cartilage, and lung in irradiated mice. *Proc Natl Acad Sci U S A* 92:4857-4861, 1995
38. Pittenger MF, Mackay AM, Beck SC: Human mesenchymal stem cells can be directed into chondrocytes, adipocytes and osteocytes. *Mol Biol Cell* 7:305a, 1996
39. Quarto R, Thomas D, Liang CT: Bone progenitor cell deficits and the age-associated decline in bone repair capacity. *Calcif Tissue Int* 56:123-129, 1995
40. Saito T, Dennis JE, Lennon DP, Young RG, Caplan AI: Myogenic expression of mesenchymal stem cells within myotubes of mdx mice in vitro and in vivo. *Tissue Eng* 1:327-343, 1995
41. Schuurman H-J, Hougen HP, van Loveren H: The rnu (Rowett Nude) and rnu^n (nznu, New Zealand Nude) rat: an update. *ILAR J* 34:3-12, 1992
42. Stevenson S, Cunningham N, Toth J, Davy D, Reddi AH: The effect of osteogenin (a bone morphogenetic protein) on the formation of bone in orthotopic segmental defects in rats. *J Bone Joint Surg [Am]* 76:1676-1687, 1994
43. Tabuchi C, Simmon DJ, Fausto A, Russell JE, Binderman I, Avioli LV: Bone deficit in ovariectomized rats: functional contribution of the marrow stromal cell population and the effect of oral dihydrotachysterol treatment. *J Clin Invest* 78:637-642, 1986
44. Takagi K, Urist MR: The role of bone marrow in bone morphogenetic protein-induced repair of femoral massive diaphyseal defects. *Clin Orthop* 171:224-231, 1982
45. Tsuji T, Hughes FJ, McCulloch CA, Melcher AH: Effects of donor age on osteogenic cells of rat bone marrow in vitro. *Mech Ageing Dev* 51:121-132, 1990
46. Wakitani S, Goto T, Pineda SJ, Young RG, Mansour JM, Caplan AI, Goldberg VM: Mesenchymal cell-based repair of large, full-thickness defects of articular cartilage. *J Bone Joint Surg [Am]* 76:579-592, 1994
47. Wakitahi S, Saito T, Caplan AI: Myogenic cells derived from rat bone marrow mesenchymal stem cells exposed to 5-azacytidine. *Muscle Nerve* 18:1417-1426, 1995
48. Werntz JR, Lane JM, Burstein AH, Justin R, Klein R, Tomin E: Qualitative and quantitative analysis of orthotopic bone regeneration by marrow. *J Orthop Res* 14:85-93, 1996
49. Wolff D, Goldberg VM, Stevenson S: Histomorphometric analysis of the repair of a segmental diaphyseal defect with ceramic and titanium fibermetal implants: effects of bone marrow. *J Orthop Res* 12:439-446, 1994
50. Wozney JM, Rosen V, Celeste AJ, Mitsock LM, Whitters MJ, Kriz RW, Hewick RM, Wang EA: Novel regulators of bone formation: molecular clones and activities. *Science* 242:1528-1534, 1988
51. Yasko AW, Lane JM, Fellinger EJ, Rosen V, Wozney JM, Wang EA: The healing of segmental bone defects, induced by recombinant human bone morphogenetic protein (rhBMP-2). *J Bone Joint Surg [Am]* 74:659-670, 1992
52. Young RG, Butler DL, Weber W, Gordon SL, Fink DJ: Mesenchymal stem cell-based repair of rabbit Achilles tendon. *Trans Orthop Res Soc* 22:249, 1997